



OPEN

Integrated metagenomics and network analysis of soil microbial community of the forest timberline

SUBJECT AREAS:

CLIMATE-CHANGE
IMPACTS

MICROBIAL ECOLOGY

FOREST ECOLOGY

Junjun Ding^{1,2}, Yuguang Zhang¹, Ye Deng^{3,4}, Jing Cong^{1,6}, Hui Lu¹, Xin Sun², Caiyun Yang⁴, Tong Yuan⁴, Joy D. Van Nostrand⁴, Diqiang Li¹, Jizhong Zhou^{2,4,5} & Yunfeng Yang²Received
9 July 2014Accepted
29 December 2014Published
23 January 2015Correspondence and
requests for materials
should be addressed to
Y.Y. (yangyf@
tsinghua.edu.cn) or
Y.Z. (zhangyg@caf.
ac.cn)

¹Institute of Forestry Ecology, Environment and Protection, and the Key Laboratory of Forest Ecology and Environment of State Forestry Administration, the Chinese Academy of Forestry, Beijing 100091, China, ²State Key Joint Laboratory of Environment Simulation and Pollution Control, School of Environment, Tsinghua University, Beijing 100084, China, ³CAS Key Laboratory of Environmental Biotechnology, Research Center for Eco-Environmental Sciences, Chinese Academy of Sciences, Beijing 100085, China, ⁴Institute for Environmental Genomics and Department of Botany and Microbiology, University of Oklahoma, Norman, OK 73019, USA, ⁵Earth Sciences Division, Lawrence Berkeley National Laboratory, Berkeley, CA 94720, USA, ⁶School of Minerals Processing and Bioengineering, Central South University, Changsha 410083, China.

The forest timberline responds quickly and markedly to climate changes, rendering it a ready indicator. Climate warming has caused an upshift of the timberline worldwide. However, the impact on belowground ecosystem and biogeochemical cycles remain elusive. To understand soil microbial ecology of the timberline, we analyzed microbial communities via 16s rRNA Illumina sequencing, a microarray-based tool named GeoChip 4.0 and a random matrix theory-based association network approach. We selected 24 sampling sites at two vegetation belts forming the timberline of Shennongjia Mountain in Hubei Province of China, a region with extraordinarily rich biodiversity. We found that temperature, among all of measured environmental parameters, showed the most significant and extensive linkages with microbial biomass, microbial diversity and composition at both taxonomic and functional gene levels, and microbial association network. Therefore, temperature was the best predictor for microbial community variations in the timberline. Furthermore, abundances of nitrogen cycle and phosphorus cycle genes were concomitant with $\text{NH}_4^+\text{-N}$, $\text{NO}_3^-\text{-N}$ and total phosphorus, offering tangible clues to the underlying mechanisms of soil biogeochemical cycles. As the first glimpse at both taxonomic and functional compositions of soil microbial community of the timberline, our findings have major implications for predicting consequences of future timberline upshift.

The forest timberline, a distinctive boundary between the continuous closed forest canopy to the treeless alpine zone^{1,2}, has solicited substantial attention because it responds quickly and markedly to climate change³. Formation of the forest timberline is typically associated with mean air temperature between 5.5 and 7.5°C during the growth season⁴, which is a major limiting factor for tree growth at high altitudes². As it has been recognized that global warming induces upshift of the timberline towards higher altitudes worldwide⁵, the sensitivity of the timberline to temperature makes the timberline a ready indicator of climate change⁶.

Several studies of the forest timberline have explored the underlying mechanisms forming spatial distribution patterns and ecological processes involved in biogeochemical cycles^{3,7}. At the global scale, temperature is a determinative factor controlling the timberline^{2,7}. At the local scale, environmental parameters and anthropogenic perturbation of the landscape affect formation of the timberline⁸. However, a majority of these studies only analyze plant communities and their responses to climatic dynamics^{9–11}. Only a few studies have analyzed microbial activities in regard to microbial biomass, carbon efflux and decomposition rates^{12–14}, neglecting microbial community composition and structure. Due to vast complexity of soil microbial communities and inadequacy of scientific tools that accurately profile microbial community structure and function¹⁵, it remains unclear whether and how the taxonomic composition and metabolic activity of microbial community are affected by timberline upshift.

The rapid development of high-throughput 16s rRNA gene sequencing has enabled fine-tuning assessment of microbial taxonomic composition¹⁶. Meanwhile, development of a functional gene microarray (GeoChip) has enabled quantitative, accurate and rapid detection of a large number of microbial genes¹⁷, making it possible to



link the metabolic potentials of microbial communities with ecosystem processes¹⁸. Aiming to obtain insights in predicting changes in microbial communities and microbe-mediated soil biogeochemical cycles for timberline upshift, we adopted 16s rRNA gene Illumina sequencing and GeoChip to analyze soil microbial communities of the coniferous forest and the shrubland, which are two vegetation belts forming the timberline in the Shennongjia national natural reserve (SNNR) located in Northwest Hubei province, China. SNNR is chosen because it is a sensitive region vulnerable to climate changes¹⁹. It is one of the most biologically diverse areas in China and a member of UNESCO's World Network of Biosphere Reserves, often known as "The Oriental Botanic Garden" and the natural bank of biological species.

Specifically, we are interested in the following scientific questions: (1) which environmental parameter best explained the formation of microbial community? and (2) were there significant linkages between microbial functional genes and soil nutrient storages, given the important role of microbes in driving biogeochemical cycles?

Results

Vegetation and soil geochemical parameters. The distance among the sampling plots within each vegetation zone ranged from 0.042–0.322 kilometers. Given the typical high soil heterogeneity, it was unsurprising to detect considerable variations in the vegetation and soil geochemical parameters, which prompted us to test for general differences between the shrubland and the coniferous forest (Table 1). We found that the number of plant species and plant diversity, calculated by Shannon index, were significantly ($P < 0.001$) higher in the coniferous forest (2.64) than in the shrubland (1.64). *Fargesia murielae* of the *Poaceae* family and *Rhododendron oreodoxa* of the *Ericaceae* family was the dominant species in the shrubland, while *Abies fargesii* of the *Pinaceae* family was the dominant species in the coniferous forest.

Many soil geochemical parameters, including soil organic carbon, labile organic carbon, dissolved organic carbon, total nitrogen, alkaline hydrolysis nitrogen, NO_3^- -N, total potassium and rapidly available phosphorus, were similar in both habitats. Soil temperature, a major limiting factor for tree growth at the forest timberline²⁰, was significantly higher ($P = 0.001$) in the shrubland than the coniferous forest. This was consistent with the annual average air temperature, which was higher in the shrubland (4.62°C) than in the coniferous forest (4.00°C). For others, total phosphorus, total sulfur, NH_4^+ -N and $\delta^{15}\text{N}$ were significantly ($P < 0.010$) higher in the shrubland, while moisture, pH, $\delta^{13}\text{C}$, Al, and Fe were significantly ($P < 0.010$) higher in the coniferous forest. These results suggested that shrubland soil was relatively richer in nutrients than the coniferous forest.

Soil microbial community of the coniferous forest and the shrubland. Microbial biomass, judged by soil microbial biomass carbon and nitrogen, were ~40% higher at the significant level of $P < 0.002$ in the shrubland than the coniferous forest (Table 1). At the taxonomic level, a total of 795,134 paired-end sequences, ranging from 14,928 to 50,849 reads per sample, were obtained from 24 samples of these two sampling sites. Finally, random re-sampling was performed with 20,000 sequences per sample, resulting in 55,440 OTUs at the 97% similarity level (Supplementary Fig. S1). The microbial taxonomic diversity, calculated by the Simpson index, was significantly ($P = 0.035$) higher in the shrubland (Table 1). At the functional gene level, 45,357 genes were detected in the shrubland samples, whereas 39,984 genes were detected in the coniferous forest samples, resulting in a significantly ($P = 0.001$) higher functional diversity in the shrubland.

To further examine differences between these two sites, Principal coordinates analysis was performed with the high-throughput sequencing and GeoChip data, respectively. Samples of the conifer-

Table 1 | Summary of environmental parameters analyzed by two-tailed *t*-test

	Shrubland	Coniferous forest	<i>P</i> value
Plant parameters			
Plant species	12 (5)	47 (17)	0.001
Plant diversity	1.64 (0.01)	2.64 (0.33)	0.001
Microbial parameters			
Taxonomic diversity	248.49 (146.37)	121.58 (130.59)	0.035
Functional diversity	126.19 (0.61)	124.18 (0.96)	0.001
Soil microbial biomass carbon (mg/kg)	1457.39 (315.10)	1081.40 (247.75)	0.002
Soil microbial biomass nitrogen (mg/kg)	169.20 (34.69)	120.34 (23.52)	0.001
Soil biogeochemical parameters			
Moisture (%)	29.73 (2.73)	45.14 (4.23)	0.001
Soil temperature (°C)	12.14 (0.35)	10.90 (0.50)	0.001
Air annual average temperature (°C)	4.62	4.00	n/a
Soil organic carbon (mg/kg)	59981.92 (12469.14)	63634.61 (16736.75)	0.793
Labile organic carbon (mg/kg)	6093.65 (2622.35)	6441.53 (3422.21)	0.782
Dissolved organic carbon (mg/kg)	283.27 (223.28)	206.90 (93.19)	0.282
Total nitrogen (mg/kg)	4447.50 (1059.86)	4311.82 (852.72)	0.564
Alkaline hydrolysis nitrogen (mg/kg)	404.51 (96.69)	350.57 (79.80)	0.092
NH_4^+ -N (mg/kg)	19.29 (3.43)	15.26 (3.32)	0.006
NO_3^- -N (mg/kg)	11.02 (5.28)	18.42 (14.44)	0.147
$\delta^{13}\text{C}$ (‰)	-25.98 (0.41)	-25.44 (0.26)	0.001
$\delta^{15}\text{N}$ (‰)	4.61 (0.82)	3.00 (0.76)	0.001
pH	4.43 (0.15)	5.07 (0.48)	0.001
Rapidly available phosphorus (mg/kg)	8.39 (0.58)	11.41 (2.58)	0.580
Total phosphorus (mg/kg)	1971.66 (1052.02)	604.50 (109.59)	0.001
Total sulfur (mg/kg)	656.67 (259.32)	337.57 (72.84)	0.001
Total potassium (mg/kg)	4281.21 (777.54)	4230.07 (1389.61)	0.739
Al (mg/kg)	22572.10 (3378.57)	32555.23 (3378.57)	0.001
Fe (mg/kg)	20766.62 (4067.16)	35420.78 (6583.12)	0.001
Altitude (m)	2748.50 (15.89)	2541.36 (55.38)	0.001

$P < 0.050$ is shown in bold. n/a: not applicable. Values in parenthesis represent standard deviation.



ous forest and the shrubland were well separated from each other in both datasets (Fig. 1), which was also verified by three non-parametric multivariate statistical tests of dissimilarity (adonis, MRPP and anosim, $P < 0.010$) (data not shown).

The linkage between the microbial community and environmental parameters. Pearson correlation analyses were carried out to identify environmental parameters linking to soil microbial biomass. Soil temperature was positively correlated with soil microbial biomass carbon (smbc) ($r = 0.54$, $P = 0.006$) and soil microbial biomass nitrogen (smbn) ($r = 0.75$, $P = 0.001$) (Fig. 2A), implying that temperature might be a key factor in determining soil microbial biomass. Soil $\text{NH}_4^+\text{-N}$ content was also positively correlated ($P = 0.002$) with smbc and smbn (Supplementary Fig. S2A). But most other environmental parameters, including soil pH and plant diversity, were not significantly ($P < 0.050$) correlated.

We proceeded further to identify key environmental parameters linking to microbial diversity. At the taxonomic level, soil temperature, but not $\text{NH}_4^+\text{-N}$, was positively correlated ($r = 0.53$, $P = 0.008$) with microbial diversity (Fig. 2B). At the functional gene level, both soil temperature (Fig. 2B) and $\text{NH}_4^+\text{-N}$ (Supplementary Fig. S2A) were positively correlated ($P < 0.050$) with microbial functional diversity. Meanwhile, microbial taxonomic and functional diversity were positively correlated ($P < 0.050$) with soil microbial biomass nitrogen (Supplementary Fig. S2B), showing a linkage between microbial biomass and diversity.

Canonical correspondence analysis (CCA) was performed to identify major environmental parameters linking to soil microbial community at the taxonomic or functional gene level. A total of 12 environmental parameters (pH, moisture, soil temperature, $\text{NH}_4^+\text{-N}$, total sulfur, total phosphorus, Al, Fe, altitude, plant diversity, $\delta^{13}\text{C}$ and $\delta^{15}\text{N}$) were selected as independent environmental parameters based on variance inflation factor analysis, resulting in significant ($P < 0.050$) CCA models (Fig. 3). Soil temperature, moisture, pH and altitude were the most important parameters shaping the microbial community since they aligned well with the first axis, which represented the major variations among microbial communities.

To single out the contribution of temperature to microbial community variations, partial Mantel test was performed to correlate the microbial community with temperature, soil parameters and plant community. For taxonomic composition of microbial community, temperature was the most important control factor with the highest R-value (Table 2). For functional gene composition of microbial

community, temperature was the only factor that was significantly correlated.

Bacterial taxa groups. All of the detected OTUs were classified as 26 bacterial phyla. Among them, *Proteobacteria*, *Acidobacteria*, *Actinobacteria* and *Verrucomicrobia* were the most abundant phyla. *Acidobacteria*, *Actinobacteria*, *Chloroflexi* and *Planctomycetes* were significantly higher in the shrubland, while *Proteobacteria* was significantly higher in the coniferous forest (Supplementary Fig. S3). *Proteobacteria*, as the most abundant phylum, was composed of α -*Proteobacteria*, β -*Proteobacteria*, δ -*Proteobacteria* and γ -*Proteobacteria*. Among all of the detected *Proteobacteria*, β -*Proteobacteria* and α -*Proteobacteria* were the most abundant, which was as high as 72.62% of all *Proteobacteria*. β -*Proteobacteria* of the coniferous forest was significantly ($P = 0.001$) and 192% higher than that of the shrubland, while α -*Proteobacteria* was significantly ($P = 0.001$) and 23% lower in the coniferous forest.

Selected gene categories of the shrubland and the coniferous forest. The response ratio analysis showed that genes associated with functional categories of organic remediation and soil benefit were significantly more abundant in the coniferous forest at the 95% confidence level (Supplementary Fig. S4). Genes associated with carbon cycle, sulfur cycle, bacterial phage, energy process and soil borne pathogen were significantly less abundant, whereas genes associated with nitrogen and phosphorus cycle remained similar. Detailed information of selected gene categories is described below.

Nitrogen (N) cycle. The total abundance of *amoA* genes associated with nitrification was higher in the coniferous forest (Fig. 4). Most of these *amoA* genes were derived from the archaea phylum of *Crenarchaeota*, known to be highly abundant in temperate acidic forest soil²¹. By contrast, total abundances of *nasA* and *nrfA* genes associated with N reduction and *nirS/nirK* genes associated with denitrification were significantly lower, suggesting a shift of microbial functional potential from ammonium biosynthesis towards nitrate biosynthesis. Consistently, the $\text{NO}_3^-\text{-N}$ content was 67.2% higher in the coniferous forest, albeit insignificantly, and the $\text{NH}_4^+\text{-N}$ content was significantly and 20.9% lower (Table 1).

We explored possible linkages between the $\text{NO}_3^-\text{-N}$ or $\text{NH}_4^+\text{-N}$ content and N cycle genes associated with $\text{NO}_3^-\text{-N}$ or $\text{NH}_4^+\text{-N}$ metabolism. The results showed that total abundances of nitrification genes (*amoA* and *hao*) were negatively correlated ($r = -0.46$, $P = 0.023$) with $\text{NH}_4^+\text{-N}$, and total abundances of denitrification genes

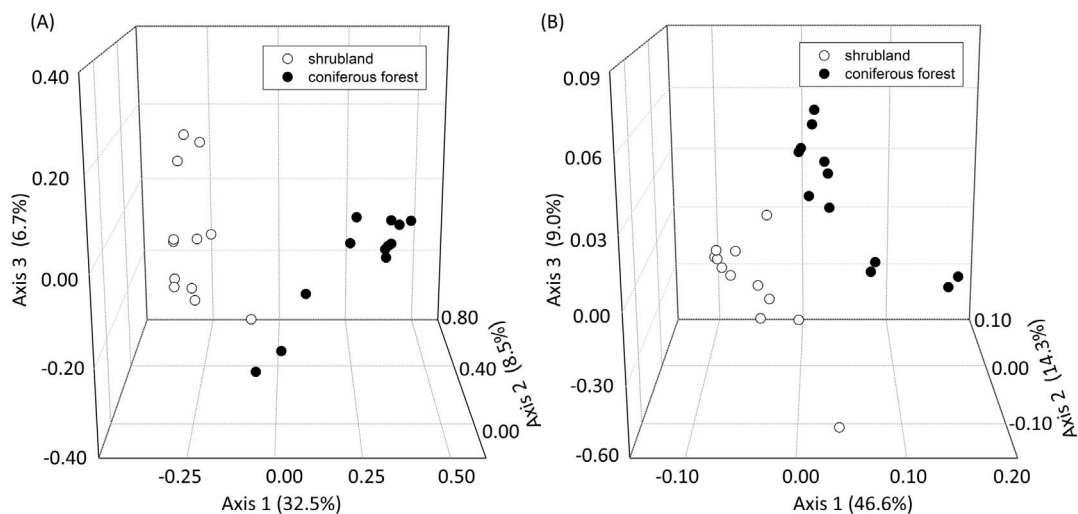


Figure 1 | Principal coordinates analysis (PCoA) of microbial community based on (A) high-throughput sequencing data and (B) GeoChip data. The values for Axes 1, 2 and 3 are percentages of variation attributed to the corresponding axis.

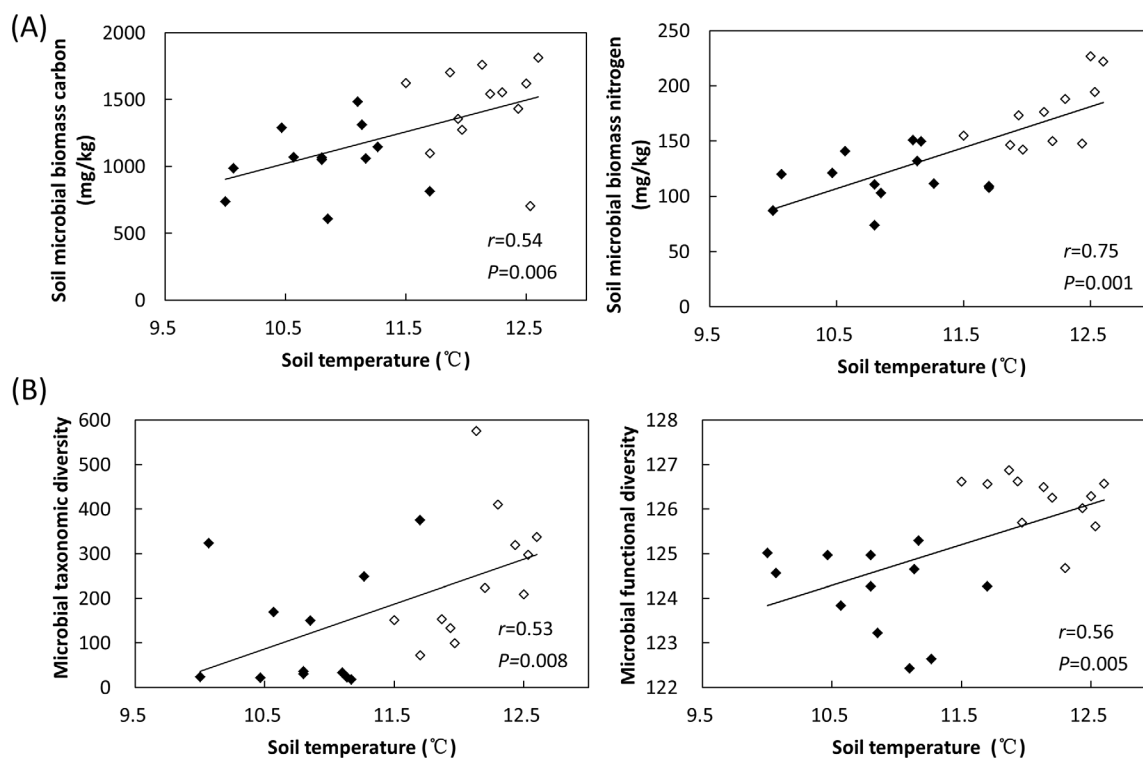


Figure 2 | Correlations between (A) microbial biomass (indicated by soil microbial biomass carbon and soil microbial biomass nitrogen) and soil temperature, and (B) microbial α -diversity (taxonomic and functional diversity) and soil temperature. White and black dots represent samples from the shrubland and the coniferous forest, respectively.

(*nirS* and *nirK*) were also negatively correlated ($r = -0.54$, $P = 0.008$) with NO_3^- -N (Supplementary Fig. S5), demonstrating that gene abundances associated with N cycle, representing microbial functional potentials, were closely linked to soil N contents.

Ammonium oxidization was controlled by a narrow group of ammonium-oxidizing archaea and bacteria²². Thus, we examined ammonium oxidizer OTUs from the sequencing data. Total abundance of the ammonium oxidizer was positively correlated to NO_3^- -N ($r = 0.49$, $P = 0.019$) and negatively correlated to NH_4^+ -N ($r = -0.41$, $P = 0.049$) (Fig. 5A), supporting the important role of ammonium oxidizer in regulating soil N cycle. To verify it, we examined bacterial *amoA* gene, which is the key functional gene of ammonium oxidizers. Similar to the observations from OTU data, total abundance of bacterial *amoA* gene was also positively correlated to NO_3^- -N ($r = 0.40$, $P = 0.057$) and negatively correlated to NH_4^+ -N ($r = -0.44$, $P = 0.033$) (Fig. 5B). Furthermore, total abundance of ammonium oxidizer was positively correlated with bacterial *amoA* gene abundance ($r = 0.38$, $P = 0.064$) (Fig. 5C).

Carbon (C) cycle. A large number of functional genes associated with fixation and degradation were detected. CODH (CO dehydrogenase) was significantly ($P = 0.050$) more abundant in the coniferous forest but *rubisco* (ribulose-1, 5-bisphosphate carboxylase/oxygenase) was less abundant, suggesting that the CODH route was a preferred C fixation route in the coniferous forest. Most of the abundant CODH genes were derived from bacteria except a few (*Sulfolobus acidocaldarius*, *Methanosarcina mazei* and uncultured *Crenarchaeote*). The most abundant CODH genes were derived from *Bradyrhizobium* sp., *Silicibacter* sp., *Aminobacter* sp., *Burkholderia* sp., *Ralstonia eutropha* *Solibacter usitatus*, *Mycobacterium smegmatis*, *Nocardioides* sp. and uncultured bacteria, which were known to have a wide distribution²³.

The total abundance of genes associated with C degradation was significantly lower in the coniferous forest samples ($P = 0.050$). Total abundances of *ara* associated with hemicellulose degradation,

acetylglucosaminidase associated with chitin degradation and *glx* associated with lignin degradation were higher in the coniferous forest, while the other genes were similar or lower (Supplementary Fig. S6A). The most abundant *glx* genes in the coniferous forest were derived from *Phanerochaete chrysosporium*, which has been well documented for its important role in lignin degradation²⁴. Despite these intrinsic differences of C fixation and degradation pathways, the net effect of C storage may be similar, as reflected in the observation that the levels of soil organic carbon and dissolved organic carbon were similar between the coniferous forest and the shrubland (Table 1).

Phosphorus (P) cycle. GeoChip 4.0 contained probes to target three P cycle genes, *ppk* (polyphosphate kinase) for polyphosphate biosynthesis, *phytase* for phytate degradation and *ppx* (exopolyphosphatase) for inorganic polyphosphate degradation. The total abundance of *ppx* genes was significantly higher in the coniferous forest, while that of *ppk* genes was significantly lower ($P < 0.050$) (Supplementary Fig. S6B). No significant difference was found for *phytase* genes. Thus, microbial functional potentials are inclined towards polyphosphate degradation, which was consistent with the higher level of rapidly available phosphorus and the lower level of total phosphorus in the coniferous forest (Table 1).

Organic remediation. Abundant organic remediation genes in the coniferous forest included genes associated with biodegradation of aromatics, chlorinated solvents, herbicides related compound, pesticides related compounds or other hydrocarbons. Among these, aromatic remediation genes were the most abundant. Consistently, more abundant aromatic components could be detected in conifer-rich sites²⁵, which might induce the aromatics remediation genes in the coniferous forest.

Correlation Networks of OTUs and functional genes. To explore possible ecological interactions of microbial communities, we used a

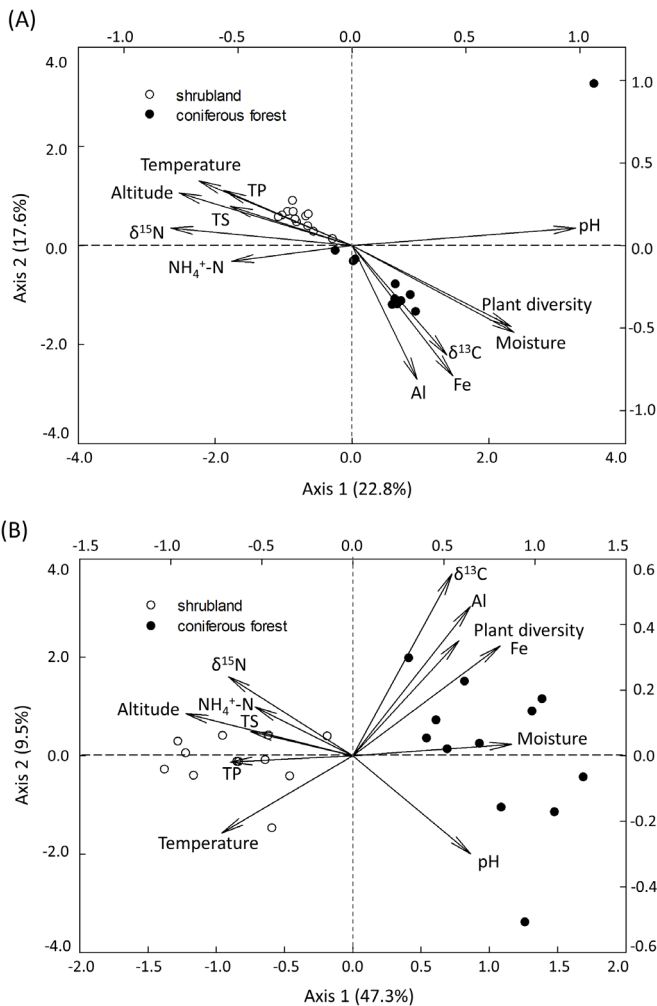


Figure 3 | Canonical correspondence analysis (CCA) of (A) high-throughput sequencing data and (B) GeoChip data with environmental parameters. TS, total sulfur; TP, total phosphorus.

random matrix theory-based algorithm²⁶ to reconstruct correlation networks from OTUs or selected GeoChip data. All of the resulting networks showed general features of ecological networks, such as scale free, small world and modular (Supplementary Table S1). At both taxonomic and functional gene levels, the coniferous forest networks had higher average connectivity and transitivity, indicative of tighter interactions/coupling within microbial communities. By contrast, the modularity, indicative of the resistance of systems to disturbance²⁷, was lower in coniferous forest networks than that of shrubland. More positive interactions, which implicated cooperation²⁸, were detected in the coniferous forest networks (98.19% in the OTU network and 92.44% in the

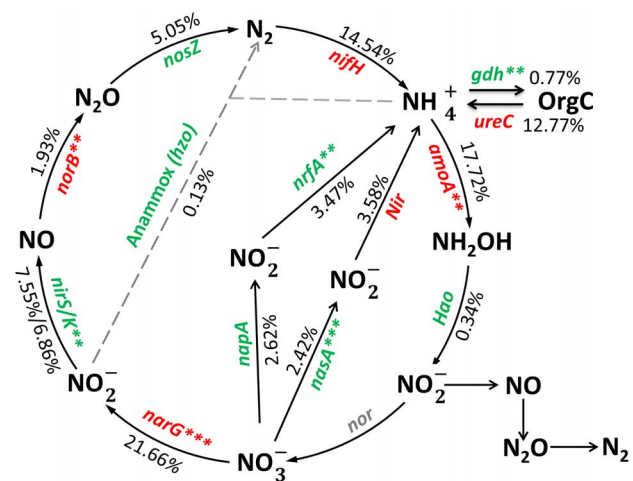


Figure 4 | The fold change of N cycle genes between the shrubland and the coniferous forest. The percentage of each gene indicated the relative fold changes, with red and green colors indicating the higher and lower signal intensity of each detected gene in the coniferous forest, respectively. This percentage was calculated by the sum of the signal intensity of each detected gene divided by the total sum of signal intensity of all detected N cycle genes, and weighted by the fold change of each gene for the coniferous forest over the shrubland. *** $P < 0.010$; ** $P < 0.050$.

GeoChip network) than those in the shrubland networks (93.24% in the OTU network and 74.79% in the GeoChip network).

Only one hub of OTU networks was detected in the shrubland and the coniferous forest, which was derived from the phylum of *Acidobacteria* and *Verrucomicrobia*, respectively (Supplementary Fig. S7A). For GeoChip networks, 25 out of 34 hub nodes of the shrubland network were C cycle genes whereas 12 out of 20 hub nodes of the coniferous forest network were N cycle genes (Supplementary Fig. S7B), which was consistent with the finding that relative abundances of C and N cycle genes were higher and lower in the shrubland samples, respectively (Supplementary Fig. S4).

To explore possible correlation between environmental factors and microbial community, we included environmental factors in our correlation network based on random matrix theory. We found that temperature was a hub node, that is, temperature was one of the nodes with the highest connectivity with other nodes (Fig. 6). Some of the directly connected nodes to temperature were among the top 10 nodes with the highest connectivity, suggesting that temperature and its directly connected nodes play an important role in maintaining the network structure and topology.

Discussion

Investigating soil microbial communities is important for understanding microbe-mediated biogeochemical cycle and ecosystem functioning²⁹. A main goal of this study is to identify the envir-

Table 2 | The relationships of microbial community structure to environmental parameters revealed by partial Mantel tests

In association with: controlling for: microbial communities	Temperature ^a		Soil ^b		Plant ^c	
	Soil	Plant	Temperature	Plant	Temperature	Soil
	$r_M(P)$	$r_M(P)$	$r_M(P)$	$r_M(P)$	$r_M(P)$	$r_M(P)$
OTUs	0.54 (0.001)	0.60 (0.001)	0.41 (0.001)	0.46 (0.001)	0.22 (0.056)	0.14 (0.094)
Functional genes	0.13 (0.031)	0.16 (0.014)	0.11 (0.215)	0.14 (0.160)	0.05 (0.375)	0.03 (0.417)

^aTemperature included soil temperature and air annual temperature.

^bSoil parameters included soil organic carbon, labile organic carbon, dissolved organic carbon, total nitrogen, alkaline hydrolysis nitrogen, $\text{NH}_4^+\text{-N}$, $\text{NO}_3^-\text{-N}$, $\delta^{13}\text{C}$, $\delta^{15}\text{N}$, soil pH, Rapidly available phosphorus, total phosphorus, total sulfur, total potassium, Al, Fe.

^cPlant parameters was the plant community structure, composed of the significant value of each specie in every sampling site.

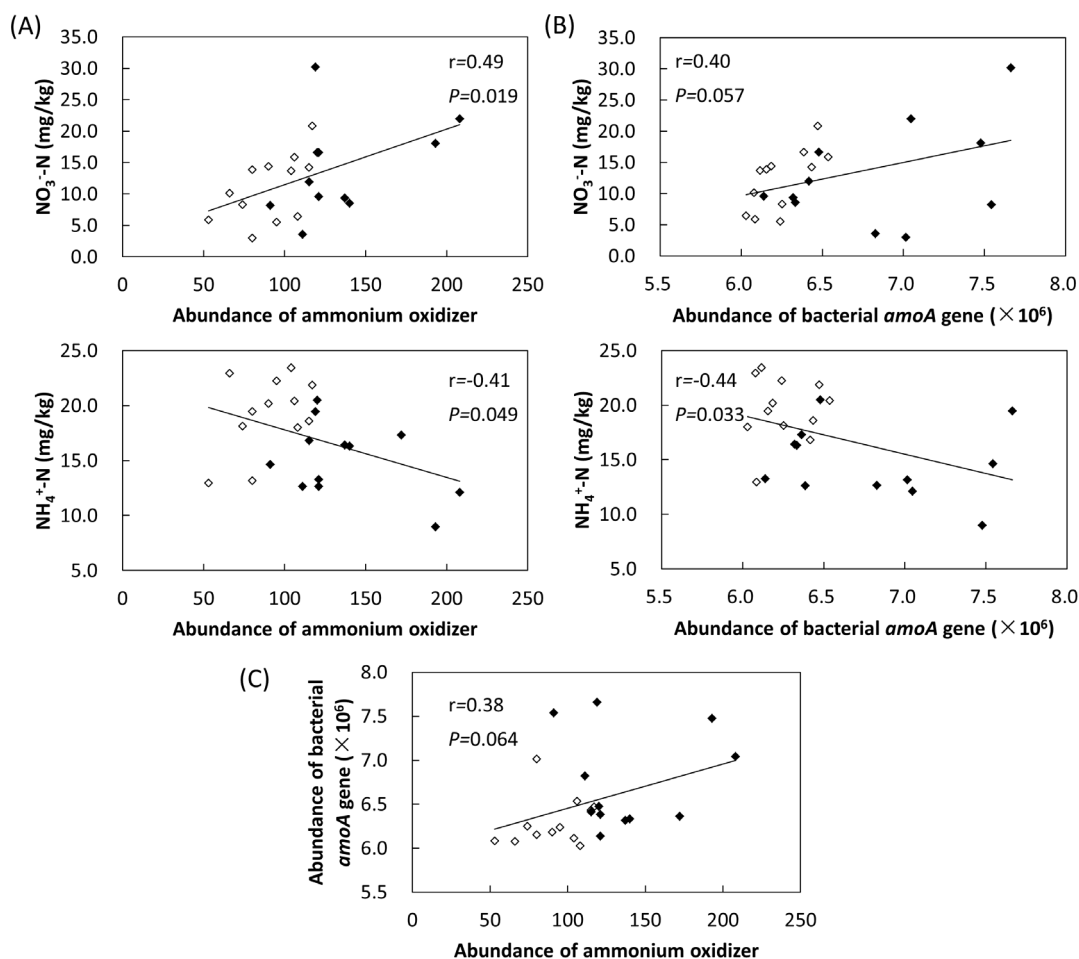


Figure 5 | Correlations between (A) $\text{NH}_4^+ \text{-N}$, $\text{NO}_3^- \text{-N}$ and total abundance of ammonium oxidizer, (B) $\text{NH}_4^+ \text{-N}$, $\text{NO}_3^- \text{-N}$ and total abundance of bacterial *amoA* gene, and (C) abundance of ammonium oxidizer and bacterial *amoA* gene. White and black dots represent samples from the shrubland and the coniferous forest, respectively.

environmental factor(s) that best explain microbial community variation. It has been proposed that above-ground plant communities drive below-ground microbial diversity³⁰. Previous studies have indicated that plants affect microbial communities via rhizodeposits and exudates and provide organic C and N to the soil microbial community^{31,32}. The different vegetation types could select for distinct soil microorganisms due to formation of a variety of microhabitats that support a diverse collection of species^{33,34}. Thus, we examined whether soil microbial functional diversity was affected by plant diversity. However, significantly higher microbial taxonomic and functional diversity were detected in the shrubland than the coniferous forest (Table 1). Considering higher plant diversity, species number and biomass in the coniferous forest, this finding suggested that plant diversity might not be the determinant of microbial diversity, which was consistent with several previous studies showing that soil microbial community was uncorrelated with plant diversity^{35–37}. The inconsistency between plant diversity and microbes could be ascribed to different ecophysiological traits of plant species, which would exert strong effects on soil biological properties^{38,39}. Thus, the plant community composition is more likely to affect soil microbial community composition than plant diversity^{35,40,41}. In addition, this could also be explained by a chance effect that a keystone species present in the plant community results in greater effects on soil processing than the contribution of the total plant diversity⁴². Notably, the dominant species were different between the shrubland and the coniferous forest. The plant litter of *Abies fargesii* in the coniferous forest with relatively higher C/N ratios provides poor

nutrients for microbial growth⁴³, and this may have a tendency to reduce microbial diversity and activity. On the contrary, *Fargesia murielae*, one of the dominant plants in the shrubland, would buffer temperature extremes and modify the local microenvironments and soil quality⁴⁴, which might be helpful for microbial survival.

Temperature has been shown to be the major factor in timberline formation⁹. Here we showed that soil temperature, among all of measured environmental parameters, showed the most significant and extensive linkages with microbial biomass, microbial diversity and composition at both taxonomic and functional gene levels. Correlation networking analysis also showed that temperature was an influential environmental parameter. Therefore, temperature was the best predictor for microbial community variations at the timberline. Our study showed that the temperature was significantly lower in coniferous forest, which was consistent with previous studies showing that the timberline forest typically had a colder temperature than its adjacent vegetation at higher altitudes^{2,45,46}, since the closed forest canopy protects the soil from sunrays and results in a lower temperature. Temperature can affect metabolic rates via the kinetics of the biological process, famously coined as “the Red Queen runs faster when she is hot”, and consequently contributes to organism differentiation and diversification^{47,48}. However, it is also possible that temperature indirectly affects microbial community by controlling soil nutrient availability, which further affects soil microbial community⁴⁹. A comparison among the shrubland, grassland, farmland and reforested land in an adjacent region to our study sites showed that the shrubland had the highest soil quality value⁵⁰.

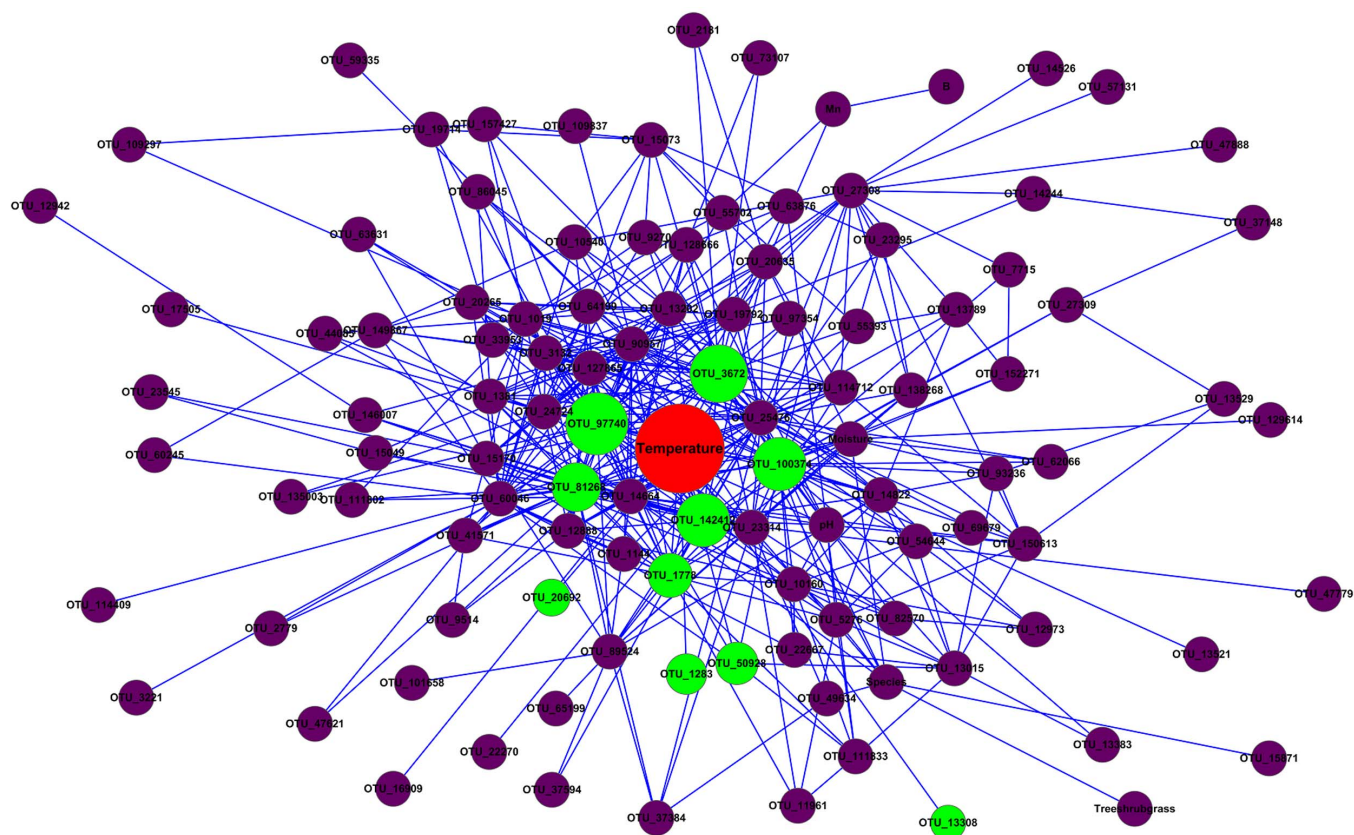


Figure 6 | Network interactions between environmental parameters and microbial taxonomic community. The red node represents temperature. The green ones represent the nodes directly connected to temperature, bigger diameter of which indicates higher connectivity. The purple ones were indirectly connected OTUs.

Similar studies on alpine ecosystems showed that treeless soil at higher altitudes had more labile C, greater microbial activity than soil of closed forest canopy^{51,52}. Consistently, higher soil nutrient contents of dissolved organic carbon, available nitrogen, total phosphorus and total sulfur in the shrubland provided a suitable environment for microbial communities, as indicated by higher microbial biomass and diversity. CCA showed that microbial community compositions were correlated with $\delta^{15}\text{N}$, total phosphorus, total sulfur; Al and Fe (Fig. 3), in addition to correlations between microbial biomass, functional diversity and $\text{NH}_4^+\text{-N}$ (Supplementary Fig. S2). Among them, N appeared to be a key factor affecting microbial community composition, diversity and productivity in many N-limited terrestrial ecosystems⁵³. The correlation between microbial biomass and $\text{NH}_4^+\text{-N}$ was consistent with previous study showing that N limitation was an influential factor in affecting microbial community⁵⁴. Meanwhile, our study showed that low microbial diversities were detected in sampling sites with high C/N ratios, which was consistent with the finding that microbial community structure and activity were negatively coupled to the soil C/N ratio⁴³. This indicated that an upward expansion of forest resulting from global warming would lead to changes in soil organic quality and the activities of the underground communities.

A parallel 16s rRNA and shotgun sequencing study on tallgrass prairies showed a strong positive correlation between taxonomic and functional gene diversity⁵⁵, suggesting a low degree of functional redundancy. By contrast, we did not detect strong correlation between overall taxonomic and functional gene diversity, which might be attributed to the differences in techniques or ecosystems. However, there was a positive correlation between bacterial *amoA* gene abundance and ammonium oxidizers (Fig. 5C), a functionally narrow group utilizing the conversion of ammonia into nitrite as the

sole energy source²². It can thus be predicted that reduction in ammonium oxidizer species is associated with decreases in the functional potential of bacterial ammonium oxidization contained within these soil communities.

Correlation networking analyses show important details of community assembly rules reflecting ecological processes such as cooperation, competition, habitat filtering and historical effects, and can represent mathematical interaction/coupling among different populations and/or functional genes that regulate system functions⁵⁶. The shorter path length and higher average connectivity and transitivity of coniferous forest networks suggested that microbial interaction/coupling was high. The high interaction might be ascribed to certain deterministic processes such as habitat filtering, reducing the spread of trait values and reflecting shared ecological tolerances⁵⁷, which was consistent with the observations of more positive interactions in the coniferous forest networks. Modularity helps control disturbances by compartmentalizing social-ecological systems⁵⁸, the higher modularity of the shrubland network indicated that the microbial system would be more resistant to changes, both at the taxonomic and functional level, which might be ascribed to higher microbial diversity of shrubland (Supplementary Table S1).

Profiling microbial communities in the habitats bordering the timberline is crucial for predicting the dynamics of microbial community changes and ecosystem functioning, since the trend of timberline upshift resulting from climate warming is likely to continue. Our results showed that temperature was the best predictor for microbial community formation and there were clear linkages between microbial functional potentials and soil biogeochemistry cycles of the timberline. Based on these results, we predict that timberline upshift resulting from global warming would cause distinct changes in microbial communities and soil C and N pools. However,



the general trend of timberline shift is modified by local, regional and temporal variations⁵⁹. It would be interesting to expand the observations in this study to other timberlines or conduct time-series experiments in order to test the generality of the observations.

Methods

Site and sampling. The study site is located at Shennongjia National Nature Reserve (SNNR, 110°14'–110°18' E, 31°26'–31°28' N) of Shennongjia Mountain, Northwest Hubei province, Central China. This area is heavily influenced by subtropical monsoon, characterized by wet (monthly precipitation > 250 mm) and hot weather in summer (monthly mean temperature > 25°C) but dry (monthly precipitation < 10 mm) and cold (monthly mean temperature < –4°C) weather in winter¹⁹. The annual mean air temperature and precipitation of this area are 7.2°C and 1500 mm, respectively. The vegetation belts forming the timberline were the shrubland and the coniferous forest. As many other landscape lines, the timberline is a well-defined boundary from a distance but a gradual transition with patchy patterns upon close inspection. To manifest differences between the shrubland and the coniferous forest, we chose typical shrubland between the altitudes of 2720 and 2776 m and the coniferous forest between the altitudes of 2456 and 2632 m to collect soil samples.

Soil samples of the shrubland and the coniferous forest were collected in August, 2011. At each site, twelve plots (20 m × 20 m) comprising typical vegetation and soil attributes were selected for sampling. At each plot, ten to fifteen soil cores at a depth of 0–10 cm were taken, mixed thoroughly and sieved with 2 mm mesh to remove roots and stones. Soil samples were kept on ice when transporting to laboratory, divided into two subsamples and stored at either 4°C for soil biogeochemical measurements or –80°C for DNA extraction.

Soil and vegetation parameter measurements. The species, number and canopy of each tree or shrub, the diameter of breast height and height of trees were surveyed at each plot. The air annual average temperature (from 1950 to 2000) was calculated with long-term records of daily air temperature by WorldClim (Version 1.4)⁶⁰. Soil temperature at each plot was measured by a Hobo Temperature instrument at the depths of 0–15 cm, respectively. The other soil geochemical parameters (soil moisture, soil pH, soil organic carbon, total nitrogen, available phosphorous, available potassium, water, dissolved organic carbon, labile organic carbon contents, $\delta^{13}\text{C}$, $\delta^{15}\text{N}$ and soil enzyme activities of cellulose, glucanase, polyphenol oxidase, sucrose and amylase) were measured as previously described⁶¹. A rapid chloroform-fumigation extraction method was used to measure soil microbial biomass carbon and nitrogen as previously described⁶². Shannon-Weaver index (H') was used to evaluate the plant diversity.

DNA extraction, purification, quantification. Soil DNA was extracted by freeze-grinding mechanical lysis as previously described⁶³. Freshly extracted DNA was purified twice using 0.5% low melting point agarose gel followed by phenol-chloroform-butanol extraction. DNA quality and quantity were assessed by the ratios of 260 nm/280 nm and 260 nm/230 nm, and final DNA contents were quantified with a PicoGreen method using a FLUO star Optima (BMG Labtech, Jena, Germany).

Illumina sequencing and data processing. 16s rDNA genes was amplified using a common primer pair targeting v4 region (Forward primer, 515F, 5'-GTGCCAGCMGCCGCGGTAA-3'; reverse primer, 806R, 5'-GGACTACHVGGGTWTCTAAT-3') combined with adapter sequences and barcode sequences^{64,65}. PCR amplification was performed in a 25 μl reaction, containing 2.5 μl 10 × AccuPrime PCR buffer II (Invitrogen, Grand Island, NY), 1 μl of each primer (10 μM), 5 μl template DNA (2 ng/ μl) and 0.1 μl AccuPrime High Fidelity Taq Polymerase. The reaction mixtures were subjected to a denaturation at 94°C for 1 min, followed by 30 cycles of 94°C for 20 s, 53°C for 25 s and 68°C for 45 s, and a final extension at 68°C for 10 min. Reactions were performed in triplicates for each sample to minimize potential biases from amplification⁶⁶. The triplicate products from the first step PCR were pooled together and purified through QIAquick Gel Extraction Kit (Qiagen, Valencia, CA), eluted in 50 μl water, and aliquoted into three PCR tubes. A second round PCR was then performed in a 25 μl reaction [2.5 μl 10 × AccuPrime PCR buffer II, 1 μl of each primer (10 μM), 0.1 μl AccuPrime High Fidelity Taq Polymerase, and 15 μl aliquot of the first-round purified PCR product] with triplicates for each sample, using phasing primers with Illumina adapters, target primers, spacers and barcodes on reverse primers. Twenty cycles of the amplifications were performed following the same program for the first round PCR. PCR products from triplicate reactions were pooled together and quantified with PicoGreen. Sample denaturation was carried out by mixing 10 μl of combined PCR products and 10 μl 0.2 N fresh NaOH. The chilled Illumina HT1 buffer was added to the denatured DNA to make a 20 pM library, which was further diluted to 15 pM by adding HT1 buffer and mixed with a PhiX DNA library. Finally, the 600 μl mixture was loaded into the MiSeq reagent cartridge and run on MiSeq (Illumina, San Diego, CA) for 2 × 250 bp paired-end sequencing.

Raw sequences were separated to samples using barcodes and with permission of up to one mismatch. Quality trimming was done using Btrim⁶⁷. Forward and reverse reads were merged into full length sequences by FLASH⁶⁸. Sequences were removed if they were too short or contained ambiguous bases. Random re-sampling was performed with 20,000 sequences per sample. The operational taxonomic units (OTUs) were classified using UCLUST at the 97% similarity level, and singletons were

removed. The taxonomic assignment was conducted by RDP classifier⁶⁹ with minimal 50% confidence estimates.

GeoChip hybridization and data processing. Purified DNA was labeled with Cy3 dye, dried, rehydrated and hybridized with GeoChip 4.0 as previously described¹⁸. After purification, GeoChip microarrays were scanned with a 100% laser power and 100% photomultiplier tube with a NimbleGen MS 200 Microarray Scanner (Roche, Basel, Switzerland), and poor-quality spots with a signal-to-noise ratio of less than 2.0 were discarded prior to statistical analyses.

Signal intensities were quantified and processed using the analysis pipeline as previously described⁷⁰. Then processed GeoChip data were analyzed using the following steps: (i) removing genes detected in no more than 5 out of 12 samples from the same vegetation type; (ii) normalizing the signal intensity of each spot by dividing the signal intensity by the total intensity of the microarray followed by multiplying by a constant; and (iii) transforming data to the natural logarithmic form.

The Simpson's reciprocal index (1/D) was used to evaluate microbial taxonomic and functional diversity. Principal coordinates analysis (PCoA) was used to determine changes of overall microbial community structure, both the high-throughput sequencing data and GeoChip data. Bray-Curtis distances were used to calculate the dissimilarity matrices from the high-throughput sequencing data and GeoChip data. Canonical correspondence analysis was used to explore linkages between microbial community structure and environmental parameters. The variance inflation factor (VIF) was used for step-wise removal of redundant parameters in CCA modeling⁷¹. Partial Mantel test was performed to correlate the microbial community (for high-throughput sequencing data, OTUs detected in more than 10 out of 24 samples was used) with the temperature, soil parameters and plant community. All of the analyses were performed by functions in the Vegan package (v.1.15–1) in R (v.3.0.1).

Network construction via the RMT-based method. Using the random matrix theory (RMT)-based method to automatically define a threshold, Pearson correlation networks were constructed from OTUs or GeoChip data as previously described. OTUs or selected functional genes (carbon and nitrogen cycle genes) detected in less than nine out of twelve replicates from the coniferous forest and the shrubland were removed to ensure reliable correlations. To explore the ecological interactions between environmental parameters and microbial community, OTUs and environmental parameters detected in less than eighteen out of twenty-four samples were removed to ensure reliable correlations. To characterize the modularity property, each network was separated into modules by the fast greedy modularity optimization. Various indices, including the average degree, average clustering coefficient, average path distance, geodesic efficiency, harmonic geodesic distance, density and transitivity, and connectedness, were used to describe overall topological properties of different networks. The topological roles of different nodes were divided into the following four subcategories by within-module connectivity (Z_i) and among-module connectivity (P_i): (i) peripheral nodes are defined as nodes with $Z_i \leq 2.5$ and $P_i \leq 0.62$; (ii) connectors are defined as nodes with $Z_i \leq 2.5$ and $P_i > 0.62$; (iii) module hubs are defined as nodes with $Z_i > 2.5$ and $P_i \leq 0.62$; and (iv) network hubs are defined as nodes with $Z_i > 2.5$ and $P_i > 0.62$.

1. Gruber, A., Pirkebner, D., Oberhuber, W. & Wieser, G. Spatial and seasonal variations in mobile carbohydrates in *Pinus cembra* in the timberline ecotone of the Central Austrian Alps. *Eur J Forest Res* **130**, 173–179 (2011).
2. Körner, C. & Paulsen, J. A world-wide study of high altitude treeline temperatures. *J. Biogeogr.* **31**, 713–732 (2004).
3. Malanson, G. P. *et al.* Mountain treelines: a roadmap for research orientation. *Arct. Antarct. Alp. Res.* **43**, 167–177 (2011).
4. Theurillat, J.-P. & Guisan, A. Potential impact of climate change on vegetation in the European Alps: a review. *Clim. Change* **50**, 77–109 (2001).
5. Panigrahy, S., Anitha, D., Kimothi, M. & Singh, S. Timberline change detection using topographic map and satellite imagery. *Trop. Ecol.* **51**, 87–91 (2010).
6. Graumlich, L. J., Waggoner, L. A. & Bunn, A. G. in *Global change and mountain regions* 501–508 (Springer, 2005).
7. Holtmeier, F. K. *Mountain timberlines*. Vol. 36 (Springer, 2009).
8. Holtmeier, F. K. & Broll, G. Sensitivity and response of northern hemisphere altitudinal and polar treelines to environmental change at landscape and local scales. *Global Ecol. Biogeogr.* **14**, 395–410 (2005).
9. Harsch, M. A., Hulme, P. E., McGlone, M. S. & Duncan, R. P. Are treelines advancing? A global meta-analysis of treeline response to climate warming. *Ecol. Lett.* **12**, 1040–1049 (2009).
10. Lingua, E., Cherubini, P., Motta, R. & Nola, P. Spatial structure along an altitudinal gradient in the Italian central Alps suggests competition and facilitation among coniferous species. *J Vet Sci* **19**, 425–436 (2009).
11. Motta, R. & Nola, P. Growth trends and dynamics in sub-alpine forest stands in the Varaita Valley (Piedmont, Italy) and their relationships with human activities and global change. *J Vet Sci* **12**, 219–230 (2001).
12. Kammer, A. *et al.* Treeline shifts in the Ural mountains affect soil organic matter dynamics. *Global Change Biol.* **15**, 1570–1583 (2009).
13. Wieser, G. & Stöhr, D. Net ecosystem carbon dioxide exchange dynamics in a *Pinus cembra* forest at the upper timberline in the central Austrian Alps. *Phyton* **45**, 233–242 (2005).



14. Withington, C. L. & Sanford Jr, R. L. Decomposition rates of buried substrates increase with altitude in the forest-alpine tundra ecotone. *Soil Biol. Biochem.* **39**, 68–75 (2007).
15. Reeve, J. R. *et al.* Effects of soil type and farm management on soil ecological functional genes and microbial activities. *ISME J* **4**, 1099–1107 (2010).
16. Shendure, J. & Ji, H. Next-generation DNA sequencing. *Nat. Biotechnol.* **26**, 1135–1145 (2008).
17. He, Z. *et al.* GeoChip: a comprehensive microarray for investigating biogeochemical, ecological and environmental processes. *ISME J* **1**, 67–77 (2007).
18. Yang, Y. *et al.* Responses of the functional structure of soil microbial community to livestock grazing in the Tibetan alpine grassland. *Global Change Biol.* **19**, 637–648 (2013).
19. Dang, H., Zhang, K., Zhang, Y., Tong, X. & Zhang, Q. Regeneration dynamics of subalpine fir (*Abies fargesii*) forest across the altitudinal range in the Shennongjia Mountains, central China. *J Plant Ecol* **6**, 36–47 (2013).
20. Alvarez-Uria, P. & Körner, C. Low temperature limits of root growth in deciduous and evergreen temperate tree species. *Funct. Ecol.* **21**, 211–218 (2007).
21. Kemnitz, D., Kolb, S. & Conrad, R. High abundance of Crenarchaeota in a temperate acidic forest soil. *FEMS Microbiol Ecol* **60**, 442–448 (2007).
22. Kowalchuk, G. A. & Stephen, J. R. Ammonia-oxidizing bacteria: a model for molecular microbial ecology. *Annu Rev Microbiol* **55**, 485–529 (2001).
23. King, G. M. & Weber, C. F. Distribution, diversity and ecology of aerobic CO₂-oxidizing bacteria. *Nat Rev Microbiol* **5**, 107–118 (2007).
24. Kersten, P. J. & Cullen, D. Cloning and characterization of cDNA encoding glyoxal oxidase, a H₂O₂-producing enzyme from the lignin-degrading basidiomycete *Phanerochaete chrysosporium*. *P Natl Acad Sci USA* **90**, 7411–7413 (1993).
25. Ussiri, D. A. & Johnson, C. E. Characterization of organic matter in a northern hardwood forest soil by ¹³C NMR spectroscopy and chemical methods. *Geoderma* **111**, 123–149 (2003).
26. Zhou, J., Deng, Y., Luo, F., He, Z. & Yang, Y. Phylogenetic molecular ecological network of soil microbial communities in response to elevated CO₂. *MBio* **2**, e00122–11 (2011).
27. Scheffer, M. *et al.* Anticipating critical transitions. *Science* **338**, 344–348 (2012).
28. Zhang, Y., Zhao, Z., Dai, M., Jiao, N. & Herndl, G. J. Drivers shaping the diversity and biogeography of total and active bacterial communities in the South China Sea. *Mol. Ecol.* **23**, 2260–2274 (2014).
29. Falkowski, P. G., Fenchel, T. & Delong, E. F. The microbial engines that drive Earth's biogeochemical cycles. *Science* **320**, 1034–1039 (2008).
30. Mitchell, R. J. *et al.* Is vegetation composition or soil chemistry the best predictor of the soil microbial community? *Plant Soil* **333**, 417–430 (2010).
31. Wardle, D. A. *Communities and Ecosystems: Linking the Aboveground and Belowground Components*. (Princeton Univ. Press, 2002).
32. Eisenhauer, N. *et al.* Plant diversity effects on soil microorganisms support the singular hypothesis. *Ecology* **91**, 485–496 (2010).
33. Faoro, H. *et al.* Influence of soil characteristics on the diversity of bacteria in the Southern Brazilian Atlantic Forest. *Appl. Environ. Microbiol.* **76**, 4744–4749 (2010).
34. Zhou, J., Xia, B., Huang, H., Palumbo, A. V. & Tiedje, J. M. Microbial diversity and heterogeneity in sandy subsurface soils. *Appl. Environ. Microbiol.* **70**, 1723–1734 (2004).
35. Broughton, L. & Gross, K. Patterns of diversity in plant and soil microbial communities along a productivity gradient in a Michigan old-field. *Oecologia* **125**, 420–427 (2000).
36. Kowalchuk, G. A., Buma, D. S., de Boer, W., Klinkhamer, P. G. L. & van Veen, J. A. Effects of above-ground plant species composition and diversity on the diversity of soil-borne microorganisms. *Anton Van Leeuw* **81**, 509–520 (2002).
37. Zak, D. R., Holmes, W. E., White, D. C., Peacock, A. D. & Tilman, D. Plant diversity, soil microbial communities, and ecosystem function: are there any links? *Ecology* **84**, 2042–2050 (2003).
38. Singh, B. K., Dawson, L. A., Macdonald, C. A. & Buckland, S. M. Impact of biotic and abiotic interaction on soil microbial communities and functions: A field study. *Appl Soil Ecol* **41**, 239–248 (2009).
39. Vries, F. T. *et al.* Abiotic drivers and plant traits explain landscape-scale patterns in soil microbial communities. *Ecol. Lett.* **15**, 1230–1239 (2012).
40. Yergeau, E., Lawrence, J. R., Waiser, M. J., Korber, D. R. & Greer, C. W. Metatranscriptomic analysis of the response of river biofilms to pharmaceutical products, using anonymous DNA microarrays. *Appl. Environ. Microbiol.* **76**, 5432–5439 (2010).
41. Zinger, L. *et al.* Global patterns of bacterial beta-diversity in seafloor and seawater ecosystems. *PLoS ONE* **6**, e24570 (2011).
42. Ladygina, N. & Hedlund, K. Plant species influence microbial diversity and carbon allocation in the rhizosphere. *Soil Biol. Biochem.* **42**, 162–168 (2010).
43. Djukic, I., Zehetner, F., Mentler, A. & Gerzabek, M. H. Microbial community composition and activity in different Alpine vegetation zones. *Soil Biol. Biochem.* **42**, 155–161 (2010).
44. He, Y., Xu, X., Kueffer, C., Zhang, X. & Shi, P. Leaf litter of a dominant cushion plant shifts nitrogen mineralization to immobilization at high but not low temperature in an alpine meadow. *Plant Soil* **383**, 415–426 (2014).
45. Körner, C., Paulsen, J. & Pelaez-Riedl, S. *A bioclimatic characterisation of Europe's alpine areas*. (Springer, 2003).
46. Hadley, J. & Smith, W. Influence of krummholz mat microclimate on needle physiology and survival. *Oecologia* **73**, 82–90 (1987).
47. Davidson, E. A. & Janssens, I. A. Temperature sensitivity of soil carbon decomposition and feedbacks to climate change. *Nature* **440**, 165–173 (2006).
48. Allen, A. P., Brown, J. H. & Gillooly, J. F. Global biodiversity, biochemical kinetics, and the energetic-equivalence rule. *Science* **297**, 1545–1548 (2002).
49. Mitchell, R. J. *et al.* Explaining the variation in the soil microbial community: do vegetation composition and soil chemistry explain the same or different parts of the microbial variation? *Plant Soil* **351**, 355–362 (2012).
50. Fu, B. J., Liu, S. L., Chen, L. D., Lv, Y. H. & Qiu, J. Soil quality regime in relation to land cover and slope position across a highly modified slope landscape. *Ecol. Res.* **19**, 111–118 (2004).
51. Sjögersten, S., Turner, B. L., Mahieu, N., Condron, L. M. & Wookey, P. A. Soil organic matter biochemistry and potential susceptibility to climatic change across the forest-tundra ecotone in the Fennoscandian mountains. *Global Change Biol.* **9**, 759–772 (2003).
52. Neff, J. C. & Hooper, D. U. Vegetation and climate controls on potential CO₂, DOC and DON production in northern latitude soils. *Global Change Biol.* **8**, 872–884 (2002).
53. Zancarini, A. *et al.* Soil nitrogen availability and plant genotype modify the nutrition strategies of *M. truncatula* and the associated rhizosphere microbial communities. *PLoS ONE* **7**, e47096 (2012).
54. Thébault, A. *et al.* Nitrogen limitation and microbial diversity at the treeline. *Oikos* **123**, 729–740 (2014).
55. Fierer, N. *et al.* Reconstructing the Microbial Diversity and Function of Pre-Agricultural Tallgrass Prairie Soils in the United States. *Science* **342**, 621–624 (2013).
56. Fuhrman, J. A. Microbial community structure and its functional implications. *Nature* **459**, 193–199 (2009).
57. Cornwell, W. K., Schwillk, D. W. & Ackerly, D. D. A trait-based test for habitat filtering: convex hull volume. *Ecology* **87**, 1465–1471 (2006).
58. Carpenter, S. R. *et al.* General resilience to cope with extreme events. *Sustainability* **4**, 3248–3259 (2012).
59. Holtmeier, F.-K. & Broll, G. Tree-line advance-driving processes and adverse factors. *Landscape Online* **1**, 1–33 (2007).
60. Hijmans, R. J., Cameron, S. E., Parra, J. L., Jones, P. G. & Jarvis, A. Very high resolution interpolated climate surfaces for global land areas. *Int J Climatol* **25**, 1965–1978 (2005).
61. Bao, S. D. Soil and agricultural chemistry analysis. *Agriculture Publication, Beijing*, 355–356 (2000).
62. Witt, C., Gaunt, J. L., Galicia, C. C., Ottow, J. C. & Neue, H.-U. A rapid chloroform-fumigation extraction method for measuring soil microbial biomass carbon and nitrogen in flooded rice soils. *Biol. Fertility Soils* **30**, 510–519 (2000).
63. Zhou, J., Bruns, M. A. & Tiedje, J. M. DNA recovery from soils of diverse composition. *Appl. Environ. Microbiol.* **62**, 316–322 (1996).
64. Caporaso, J. G. *et al.* Global patterns of 16S rRNA diversity at a depth of millions of sequences per sample. *P Natl Acad Sci USA* **108**, 4516–4522 (2011).
65. Caporaso, J. G. *et al.* Ultra-high-throughput microbial community analysis on the Illumina HiSeq and MiSeq platforms. *ISME J* **6**, 1621–1624 (2012).
66. Zhou, J. *et al.* Reproducibility and quantitation of amplicon sequencing-based detection. *ISME J* **5**, 1303–1313 (2011).
67. Kong, Y. Btrim: a fast, lightweight adapter and quality trimming program for next-generation sequencing technologies. *Genomics* **98**, 152–153 (2011).
68. Magoc, T. & Salzberg, S. L. FLASH: fast length adjustment of short reads to improve genome assemblies. *Bioinformatics* **27**, 2957–2963 (2011).
69. Wang, Q., Garrity, G. M., Tiedje, J. M. & Cole, J. R. Naive Bayesian classifier for rapid assignment of rRNA sequences into the new bacterial taxonomy. *Appl. Environ. Microbiol.* **73**, 5261–5267 (2007).
70. He, Z. *et al.* GeoChip 3.0 as a high-throughput tool for analyzing microbial community composition, structure and functional activity. *ISME J* **4**, 1167–1179 (2010).

Acknowledgments

This research was supported by grants to Yuguang Zhang from the public welfare project of the national scientific research institution (CAFRIFEEP201101), to Yunfeng Yang from Major Science and Technology Program for Water Pollution Control and Treatment (2013ZX07315-001-03), the Strategic Priority Research Program of the Chinese Academy of Sciences (XDB15010102), the National Key Basic Research Program of China (2013CB956601), National High Technology Research and Development Program of China (2012AA061401) and National Science Foundation of China (41471202 & 41171201), to Ye Deng from State Key Laboratory of Forest and Soil Ecology (Grant No. LFSE2014-02) and the Strategic Priority Research Program of the Chinese Academy of Sciences (Grant XDB15010302), and to Jizhong Zhou from the US National Science Foundation (EF-1065844).

Author contributions

Y.Y., Y.Z., J.Z. and D.L. designed experiments. J.D. and Y.Y. wrote the main manuscript text. J.D., Y.D. and X.S. analyzed the data. J.C., H.L., C.Y., T.Y. and J.V.N. performed the experiments. All authors reviewed the manuscript.



Additional information

Data Accession Microarray data have been deposited to GEO databases (<http://www.ncbi.nlm.nih.gov/geo/query/acc.cgi?acc=GSE58433>). Sequencing data are currently being deposited to GEO databases.

Supplementary information accompanies this paper at <http://www.nature.com/scientificreports>

Competing financial interests: The authors declare no competing financial interests.

How to cite this article: Ding, J. *et al.* Integrated metagenomics and network analysis of soil microbial community of the forest timberline. *Sci. Rep.* 5, 7994; DOI:10.1038/srep07994 (2015).



This work is licensed under a Creative Commons Attribution-NonCommercial-NoDerivs 4.0 International License. The images or other third party material in this article are included in the article's Creative Commons license, unless indicated otherwise in the credit line; if the material is not included under the Creative Commons license, users will need to obtain permission from the license holder in order to reproduce the material. To view a copy of this license, visit <http://creativecommons.org/licenses/by-nc-nd/4.0/>